Development 139, 2161-2169 (2012) doi:10.1242/dev.075069

RBE controls microRNA164 expression to effect floral organogenesis

Tengbo Huang[1], Francesc López-Giráldez[2], Jeffrey P. Townsend[2] and Vivian F. Irish[1,2,*]

SUMMARY

The establishment and maintenance of organ boundaries are vital for animal and plant development. In the *Arabidopsis* flower, three microRNA164 genes (*MIR164a*, *b* and *c*) regulate the expression of *CUP-SHAPED COTYLEDON1* (*CUC1*) and *CUC2*, which encode key transcriptional regulators involved in organ boundary specification. These three miR164 genes are expressed in distinct spatial and temporal domains that are crucial for their function. Here, we show that the C2H2 zinc finger transcriptional repressor encoded by *RABBIT EARS* (*RBE*) regulates the expression of all three miR164 genes. Furthermore, we demonstrate that RBE directly interacts with the promoter of *MIR164c* and negatively regulates its expression. We also show that the role of RBE in sepal and petal development is mediated in part through the concomitant regulation of the *CUC1* and *CUC2* gene products. These results indicate that one role of RBE is to fine-tune miR164 expression to regulate the *CUC1* and *CUC2* effector genes, which, in turn, regulate developmental events required for sepal and petal organogenesis.

KEY WORDS: *Arabidopsis*, miRNA, Flower development

INTRODUCTION

The formation of boundaries between different cell populations is crucial for development. Such boundaries, in addition to delineating identity, often act as organizing centers to regulate downstream signaling events (Dahmann et al., 2011). In *Arabidopsis*, a subset of NAM-ATAF-CUC (NAC) domain transcription factors plays a central role in the establishment and maintenance of organ boundaries. These partially redundant gene products are expressed at boundaries, and their loss of function results in organ fusions and defects in both vegetative and floral development (Aida et al., 1997; Aida et al., 1999; Aida and Tasaka, 2006; Takada et al., 2001; Vroemen et al., 2003). Two such NAC domain genes, *CUC1* and *CUC2*, are post-transcriptionally regulated by microRNA164 (miR164) (Baker et al., 2005; Laufs et al., 2004; Mallory et al., 2004; Rhoades et al., 2002; Sieber et al., 2007). Negative regulation by miR164 fine-tunes the levels, as well as patterns of expression, of the *CUC1* and *CUC2* transcripts. Precise regulation of *CUC1* and *CUC2* transcript accumulation is crucial for proper control of organ number and boundary formation throughout vegetative and reproductive development (Baker et al., 2005; Laufs et al., 2004; Mallory et al., 2004; Sieber et al., 2007).

The microRNA miR164 is transcribed from three loci: *MIR164a*, *MIR164b* and *MIR164c* (Bonnet et al., 2004; Jones-Rhoades and Bartel, 2004; Reinhart et al., 2002; Wang et al., 2004). These genes exhibit partial functional redundancy, particularly in flower development (Baker et al., 2005; Sieber et al., 2007). Loss of function of the *MIR164c* gene, also known as *EARLY EXTRA PETALS1* (*EEP1*), results in the growth of extra petals due to the failure to properly repress *CUC1* and *CUC2* in the second whorl (Baker et al., 2005). In the *mir164abc* triple mutant, the floral defects exhibited by *eep1* are enhanced. Nevertheless, the *mir164a* and *mir164b* single mutants do not show obvious floral phenotypes (Sieber et al., 2007). These observations indicate that the miR164 genes are functionally redundant, yet differences in their expression patterns and mutant phenotypes imply that they have unique roles as well. As a consequence, deciphering the precise regulation of the spatial and temporal domains of miR164 gene expression is pivotal to revealing the functions of these microRNAs in organ boundary formation.

The gene *RABBIT EARS* (*RBE*) has been postulated to be involved in defining second whorl boundaries, and is specifically expressed in petal primordia during early stages of petal development (Krizek et al., 2006; Takeda et al., 2004; reviewed in Irish, 2008). *RBE* encodes a putative C2H2 zinc finger transcriptional repressor and, thus, is likely to function as a negative regulator (Takeda et al., 2004). Loss-of-function *rbe* mutants exhibit loss of or aberrant petals, as well as fused sepals (Krizek et al., 2006; Takeda et al., 2004). Interestingly, these morphological defects resemble the phenotypes observed in *cuc1 cuc2* double mutants (Aida et al., 1997) and in *35S:MIR164b* transgenic plants (Baker et al., 2005; Laufs et al., 2004; Mallory et al., 2004; Rhoades et al., 2002; Sieber et al., 2007), implying that *RBE* might function in regulating miR164-mediated processes.

In this study, we examine the role of *RBE* in the miR164-CUC pathway in *Arabidopsis* sepal and petal development. We demonstrate that RBE binds to the promoter of *MIR164c* and represses its transcription. Genetic analyses also support the idea that RBE negatively regulates the expression of *MIR164c*. In addition, we also demonstrate that RBE regulates the expression of the other two miR164 genes. Thus, RBE coordinately regulates the appropriate expression of the miR164 genes, which in turn impacts the expression of the CUC1 and CUC2 transcription factors.

MATERIALS AND METHODS

Genetic stocks and growth conditions

Arabidopsis thaliana plants were grown at 22°C under 16-hour light/8-hour dark conditions. The *rbe-2* (Salk_037010), *rbe-3*, *mir164b-1* (Salk_136105), *cuc1-1* and *cuc2-1* seeds were obtained from the *Arabidopsis* Biology Resource Center (ABRC). *mir164a-4* (GABI

[1]Department of Molecular, Cellular and Developmental Biology, Yale University, New Haven, CT 06520-8104, USA. [2]Department of Ecology and Evolutionary Biology, Yale University, New Haven, CT 06520-8106, USA.

*Author for correspondence (vivian.irish@yale.edu)

Accepted 4 April 2012

867E03) was obtained from Nottingham *Arabidopsis* Stock Center (NASC). *eep1* (also referred to as *mir164c-1*) was a gift from Dr Elliot Meyerowitz (California Institute of Technology, Pasadena, CA, USA). *mir164a-4* and *mir164b-1* were in the Columbia (Col-0) background. All the other mutants are in the Landsberg *erecta* (L *er*) background. Double mutants were confirmed by genotyping. Methods for genotyping *mir164b-1* and *eep1* have been described previously (Mallory et al., 2004). *rbe-2* was genotyped using primers RBE5C2 and LBb1 to amplify a 400 bp genomic fragment, whereas the wild-type allele was identified by primers RBE5C2 and RBEO3 producing a 388 bp product. *rbe-3* was identified by derived cleaved amplified polymorphic sequence (dCAPS) (Neff et al., 1998) using primers RBE3GF2 and RBEO3 and followed by the digestion of PCR products with *Sal*I (New England BioLabs, Ipswich, MA, USA), producing two fragments (151 bp and 23 bp) in L *er* and one fragment (174 bp) in *rbe-3*. In the other crosses with *rbe-3*, except *mir164a rbe-3*, homozygous *rbe-3* plants were selected by phenotype and subsequently genotyped. Methods to genotype *cuc1-1* and *cuc2-1* have been reported previously (Takada et al., 2001). Primers used in genotyping were (5′-3′): LBb1, CAAACCAGCGTGGACCGCTTGCTGCAACTC; RBE5C2, TTTATTTTGGCCGTTTAGGGAAGA; RBE3GF2, GCCACACCTCCTGAATGTGATCGTCGA; RBEO3, GACTTCACCATTGTCATGTTCATATCT; RBE, ATGATGGATAGAGGAGAATGCTTGATG; RBE2, AGCTAGTTAACCTTAGGCG. Transgenic *pCUC1:CUC1*, *pCUC1:CUC1*^{m}, *pCUC2:CUC2* and *pCUC2:CUC2*^{m} are all in the L *er* background and obtained from the ABRC. These lines were individually crossed with *rbe-3*. *rbe-3* plants with the *CUC1/2* or *CUC1*^{m}*/2*^{m} transgene were identified in the F2 population by screening seedlings on BASTA and genotyping for *rbe-3*.

GUS reporter lines *pMIR164a:GUS* and *pMIR164b:GUS* (Raman et al., 2008) were kindly provided by Dr Patrick Laufs (Institut National de la Recherche Agronomique, France). These two lines were originally in Col-0 background and were backcrossed twice into L *er*. These backcrossed lines were crossed to *rbe-3* and mutant plants containing the GUS reporter were identified from the F2 population. *pMIR164c:GUS* (Baker et al., 2005) and *pMIR164c:3XVENUS-N7* (Sieber et al., 2007) were gifts from Dr Elliot Meyerowitz (California Institute of Technology, Pasadena, CA, USA).

Transgenic plants

To make *35S:GR-RBE*, the *RBE* coding region was amplified from L *er* genomic DNA using primers RBE and RBE2 (see above). The PCR product was first cloned into the pCR8 vector (Invitrogen, Carlsbad, CA, USA) and subcloned into the *pJAN33* plasmid (a gift from Dr Kathy Barton, Carnegie Institute, Palo Alto, CA, USA) using the GATEWAY cloning strategy (Invitrogen, Carlsbad, CA, USA). The resulting *pJAN33-RBE* plasmid was transformed into *Arabidopsis* plants using the floral dip method (Clough and Bent, 1998) and transformants were selected on BASTA. *pJAN33* contains the CaMV 35S promoter upstream of a GATEWAY cassette fused to a GR tag and a FLAG tag at the N-terminus, so the *pJAN33-RBE* transgenic plants ubiquitously express a double-tagged RBE protein (GR-FLAG-RBE).

Dexamethasone (DEX) induction and total RNA extraction

pJAN33-RBE floral buds were treated with DEX (10 μM dexamethasone, 0.1% ethanol, 0.015% silwet) or mock (0.1% ethanol, 0.015% silwet) solution for four hours. After the treatments, floral tissues were harvested, frozen in liquid nitrogen and stored at –80°C. Total RNA was extracted with Trizol (Invitrogen) according to the manufacturer's instructions, treated with TURBO DNase (Applied Biosystems, Carlsbad, CA, USA), purified using the Rneasy kit (Qiagen, Valencia, CA, USA), and used in subsequent analyses.

RNA-seq analysis

Eight sequencing libraries (two biological replicates, each with two technical replicates for four-hour DEX- or mock-treated floral tissues) were produced from purified total RNA samples by standard Illumina protocols. The libraries were run on eight lanes of an Illumina Genome Analyzer, generating an average of 27,650,720 single-end reads of 36 bp each. We used Tophat v1.2.0 (Trapnell et al., 2009) (http://tophat.cbcb.umd.edu/) to perform spliced alignments of the reads against the *Arabidopsis thaliana* TAIR10 reference genome (http://www.arabidopsis.org/). Only reads that mapped to a single unique location within the genome with a maximum of two mismatches in the anchor region of the spliced alignment were reported in these results. We used the default settings for all other *Tophat* options. To obtain a tally of the number of the reads that overlapped the exons of a gene, we analyzed the aligned reads with HTSeq v0.4.5p6 (unpublished; http://www-huber.embl.de/users/anders/HTSeq/doc/) and the gene structure annotation file for the reference genome (TAIR10 gff file; downloaded from http://www.arabidopsis.org/). The tally for each sample was then processed with LOX v1.6 (Zhang et al., 2010) to analyze gene expression levels statistically. Data have been deposited in the Gene Expression Omnibus database under accession number GSE36469.

qRT-PCR

Total RNA from L *er*, *rbe-3* and DEX- or mock-treated *pJAN33-RBE* floral tissues were extracted as described above and purified using TURBO DNA-free Kit (Applied Biosystems). qRT-PCR of mRNA transcripts was performed using Multiscribe reverse transcriptase (Applied Biosystems) and Taqman gene expression assay (Applied Biosystems) according to the manufacturer's instructions. For qRT-PCR of *miR164a/b*, reverse transcription was carried out using stem-loop primers (Chen et al., 2005) and *miR164a/b* was quantified using the Taqman miRNA assay (Applied Biosystems). Changes in gene expression were calculated from three biological replicates using $2^{-\Delta\Delta Ct}$ method. For mRNA quantification, the relative RNA levels were normalized to the value of *ACTIN 2* (*ACT2*). For miRNA quantification, expression level of snoR66 was used as the standard for normalization.

Histology, confocal imaging and scanning electron microscopy

β-Glucuronidase (GUS) staining was carried out as published previously (Nakayama et al., 2005) with minor modifications. Whole inflorescences were collected, vacuum infiltrated for 15 minutes and incubated at 37°C in GUS staining solution (2 mM X-glucuronic acid, 50 mM sodium phosphate buffer, pH 7.2, 10 mM EDTA, pH 8, 0.1% Triton X-100, 6 mM FeCN). owing to the different promoter activities of three miR164 genes, we used different incubation times in this step. In both L *er* and *rbe-3*, we used 12 hours for *pMIR164a:GUS*, 3 hours for *pMIR164b:GUS* and 24 hours for *pMIR164c:GUS*. For whole mounts, floral tissues were cleared using an ethanol series, mounted in 30% glycerol; for sectioned material, cleared floral tissues were embedded in Paraplast (Fisher Scientific, Pittsburgh, PA, USA) and sectioned at 8 μm. Whole mounts and sectioned material were examined using a Zeiss Axiophot microscope. For confocal imaging, floral tissues were stained with FM4-64 (Invitrogen), mounted in water and imaged using a Zeiss LSM 510 confocal microscope. For scanning electron microscopy, tissues were fixed overnight in formalin/acetic acid/alcohol fixative with subsequent dehydration in an ethanol series. Samples were critical-point dried and sputter coated in gold/palladium and imaged using an ISI SS40 scanning electron microscope.

Chromatin immunoprecipitation (ChIP)

pJAN33-RBE floral tissues treated with 4-hour DEX or mock solution were harvested, washed with de-ionized water and crosslinked with 1% formaldehyde. Crosslinking was quenched with 0.125 M glycine. Procedures for nuclear extracts and immunoprecipitation were adapted from Gendrel et al. (Gendrel et al., 2002), with modifications. Sonications of nuclear extracts were performed at 4°C for 15 minutes (power level 5; Diagenode, Denville, NJ, USA). After chromatin shearing, 6 μl anti-FLAG monoclonal antibody (Sigma-Aldrich, St Louis, MO, USA) was added to each sample to immunoprecipitate GR-FLAG-RBE proteins. After reversing crosslinks, DNA was purified by phenol:chloroform extraction, ethanol precipitated, and resuspended in 50 ml TE. Two microliters of immunoprecipitated DNA was used in qPCR (*MIR164c* promoter) or semi-quantitative PCR (*MIR164a* and *MIR164b* promoter). The exon region of *APETALA3* (*AP3*) was used as the negative control. Primers used for PCR are listed in supplementary material Table S2. qRT-PCR utilized Power SYBR Green PCR Master Mix (Applied Biosystems) for amplification. Semi-quantitative PCR conditions were: 33 cycles, 94°C for 30 seconds,

55°C for 30 seconds and 72°C for 30 seconds. DNA band intensity was measured using ImageJ. The abundance ratio of a specific promoter fragment in DEX- versus mock-treated ChIP samples was first normalized to the negative-control gene *AP3*, then was divided by the normalized ratio of DEX- to mock-treated input values to obtain a fold enrichment. Three biological replicates were carried out for each ChIP experiment.

RESULTS

RBE binds to the *MIR164c* promoter and represses its expression in the flower

To investigate the function of RBE in floral organ and boundary formation, we constructed an inducible form of RBE by fusing its coding region to the glucocorticoid receptor ligand binding domain sequence (*GR*). Transgenic plants expressing *GR-RBE* under the regulation of the strong constitutive *35S* promoter were morphologically normal (supplementary material Fig. S1). However, treatment with 10 μM dexamethasone (DEX) every other day for 20 days resulted in *35S:GR-RBE* plants becoming stunted and having epinastic rosette leaves (supplementary material Fig. S1). Striking phenotypes were also found in the reproductive phase. DEX-treated *35S:GR-RBE* plants had compact inflorescences with short underdeveloped sepals, petals and stamens (Fig. 1A-D). The carpels of such plants were short and swollen and fertility was highly reduced. These defects resembled the miR164-resistant $CUC1^m$ and $CUC2^m$ overexpression phenotypes (Baker et al., 2005), which suggests that RBE is a regulator of the miR164-CUC pathway. Furthermore, because RBE is a putative transcriptional repressor, it probably acts upstream of one or more of the miR164 genes and negatively regulates their expression.

To identify targets of RBE action, we carried out whole-transcriptome RNA-seq analyses to compare gene expression in four-hour DEX and mock-treated *35S:GR-RBE* young floral buds. We focused on the 832 genes expression of which was significantly reduced ($P<0.025$) by twofold or more in DEX compared with mock-treated plants. In this analysis, we identified *MIR164c* (*EEP1*) as a candidate target of *RBE*. *MIR164c* expression was strongly repressed, with no matching reads after 4-hour DEX treatment (supplementary material Table S1). This result was confirmed by quantitative PCR in which *MIR164c* expression was ~30-fold decreased in 4-hour DEX versus mock-treated samples (Fig. 1E).

To determine whether RBE directly binds to *MIR164c* promoter sequences, we performed chromatin immunoprecipitation (ChIP) on 4-hour mock- and DEX-treated *35S:GR-RBE* floral tissues. After immunoprecipitation, semi-quantitative PCR and qPCR were utilized to amplify three fragments in the 1000 bp region upstream of the transcription start site of *MIR164c* (Nikovics et al., 2006). Both approaches resulted in an approximately threefold enrichment of the same fragment specifically in DEX-treated floral tissues (Fig. 1F,G), indicating that RBE is associated with *MIR164c* promoter sequences.

RBE regulates *MIR164c* expression patterns and levels in floral organs

To determine how RBE regulates *MIR164c* expression, we examined the expression of *pMIR164c:GUS* in both wild-type (L *er*) and *rbe-3* floral buds. Flowers containing the *pMIR164c:GUS* transgene in the L *er* background displayed an expression pattern of *MIR164c* based on GUS staining that was similar to that reported in previous studies (Baker et al., 2005; Sieber et al., 2007). Prior to stage 5, *MIR164c* promoter activity was observed in the inflorescence meristem, floral meristem and the regions between

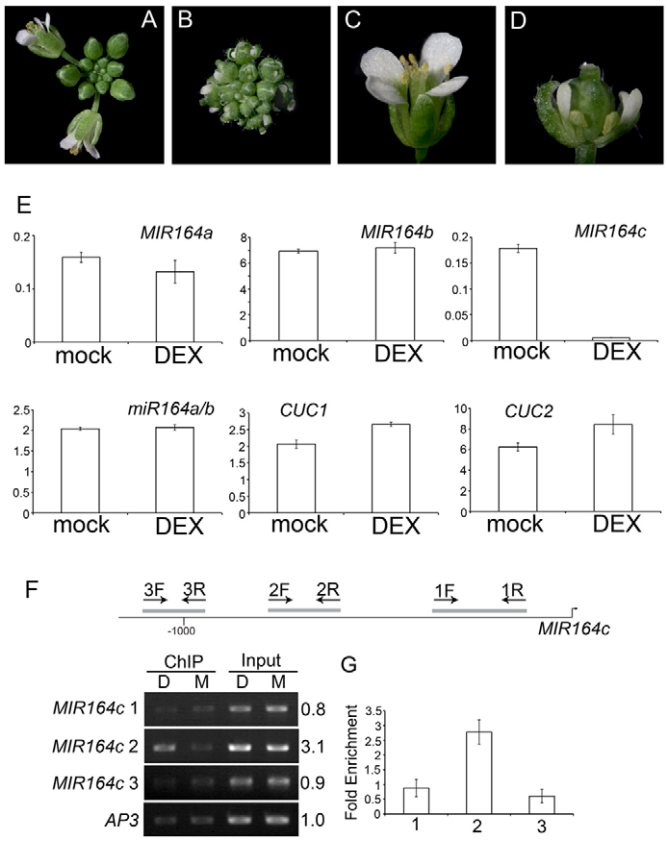

Fig. 1. RBE directly regulates *MIR164c*. (**A-D**) Inflorescence and flower of *35S:GR-RBE* mock- (A,C) and DEX- (B,D) treated *Arabidopsis* plants. DEX-treated *35S:GR-RBE* plants have a compact inflorescence and short floral organs. (**E**) Levels of *MIR164a*, *MIR164b* and *MIR164c* transcripts, mature *miR164a/b* and *CUC1*, *CUC2* expression assessed by qRT-PCR in 4-hour DEX and 4-hour mock treated *35S:GR-RBE* plants. Note that *MIR164c* levels are significantly reduced in the DEX treatment. The *y*-axis shows relative RNA levels normalized to the value of *ACT2*. (**F**) ChIP assays show direct interaction of RBE with the promoter of *MIR164c*. Semi-quantitative PCR employing three sets of primers (arrows) to amplify three fragments (gray bars) in the 1000 bp upstream of the transcription start site. Band intensity ratios (DEX/mock), after normalizing by input and the control gene (*AP3*), are indicated at right. Fragment 2 is enriched in 4-hour DEX- (D) versus 4-hour mock- (M) treated samples. (**G**) qPCR analysis of ChIP products. qPCR primers were designed to recognize sequences included within each *MIR164c* promoter fragment shown in F. Note that fragment 2 shows approximately threefold enrichment, consistent with the semi-qPCR result. Error bars represent s.e.m.

adjacent sepals (Fig. 2C,M,N; supplementary material Fig. S2). The expression of a *pMIR164c:3XVENUS-N7* construct (Sieber et al., 2007) also showed a similar but weaker pattern of *MIR164c* promoter activity in early stage floral primordia (supplementary material Fig. S3). *MIR164c* was also expressed in the gynoecium and petal primordia during stages 5-7 (Fig. 2O; supplementary material Fig. S2). In late stage flowers, *MIR164c* expression was detected primarily in the sepals and in the septum of the gynoecium (supplementary material Fig. S2). In transgenic flowers in the *rbe-3* background, the overall expression pattern of *pMIR164c:GUS* was similar to that of wild type, particularly after stage 5 (Fig. 2F,P-R; supplementary material Fig. S2). However, GUS staining was more intense in young floral buds, especially during stages 3-

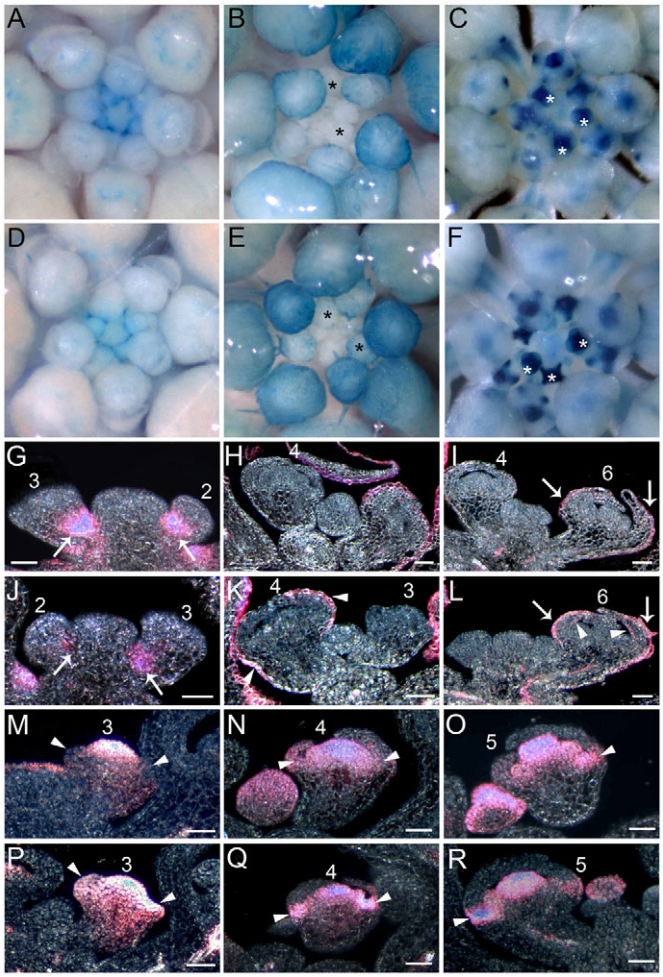

Fig. 2. Spatial and temporal expression patterns of miR164 genes in wild-type and *rbe-3 Arabidopsis* plants. (**A-F**) Whole-mount staining of *pMIR164a:GUS* in L *er* (A) and *rbe-3* (D); *pMIR164b:GUS* in L *er* (B) and *rbe-3* (E); and *pMIR164c:GUS* in L *er* (C) and *rbe-3* (F). Note that *pMIR164a:GUS* expression is reduced in early stage flowers of *rbe-3* and *pMIR164b:GUS* expression is detected prematurely in stage 4-5 flowers (black asterisks in B and E) in *rbe-3*. The *pMIR164c:GUS* spatial pattern is similar in L *er* and *rbe-3*, but appears to be more intense in *rbe-3* particularly in stage 3-5 flowers (white asterisks in C and F). (**G-R**) Longitudinal sections show *pMIR164a:GUS* patterns in L *er* (G) and *rbe-3* (J); *pMIR164b:GUS* patterns in L *er* (H,I) and *rbe-3* (K,L); and *pMIR164c:GUS* patterns in L *er* (M-O) and *rbe-3* (P-R). Note that *pMIR164a:GUS* expression is reduced in stage 2 and 3 flowers in *rbe-3* (arrows in J) compared with those in L *er* (arrows in G). *pMIR164b:GUS* is expressed on the abaxial side of sepals in *rbe-3* (arrowheads in K) but not in L *er* (H and I) at stage 4. At stage 6, *pMIR164b:GUS* expression appears on the abaxial side of sepals in L *er* (arrows in I), whereas in *rbe-3* (L), *pMIR164b:GUS* expression is observed on both the abaxial side (arrows) and adaxial side (arrowheads) of sepals. *pMIR164c:GUS* expression is stronger in the sepal primordia in *rbe-3* (arrowheads in P) relative to L *er* (M). At stage 4 and 5, *pMIR164c:GUS* expression appears to be increased in *rbe-3* relative to L *er*, specifically in the petal primordia (arrowheads in O and R) and their precursor cells (arrowheads in N and Q). Floral stages are labeled above the flowers. Scale bars: 100 μm.

5, and in stage 3 sepal primordia and stage 4-5 petal primordia (Fig. 2F,P-R). Although overall expression levels were weaker for the *pMIR164c:3XVENUS-N7* construct, GFP signal was somewhat more intense in early stage *rbe-3* floral primordia compared with WT (supplementary material Fig. S3). These results were consistent with the qRT-PCR results using whole inflorescence tissue, in that *MIR164c* expression was mildly but significantly increased in the *rbe-3* relative to L *er* backgrounds (Fig. 3), and suggests that *RBE* represses *MIR164c* in a stage-specific manner.

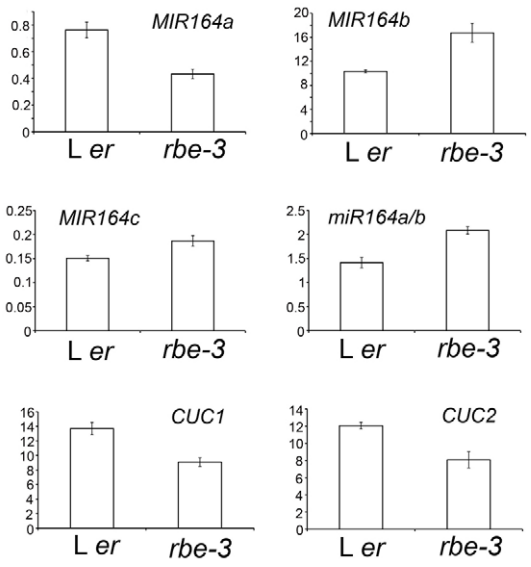

Fig. 3. Levels of primary and mature miR164, *CUC1* and *CUC2* transcripts in the whole inflorescences of L *er* and *rbe-3*. Quantification of primary and mature miR164, as well as *CUC1* and *CUC2* expression in L *er* and *rbe-3* using qRT-PCR. The *y*-axis represents relative RNA levels of each primary transcript or the mature *miR164a/b*, normalized to internal controls (*ACT2* for mRNA and *snoR66* for miRNA). Each result represents three biological replicates. Error bars represent s.e.m.

RBE functions largely through regulating *MIR164c* expression

Plants mutant for *rbe-3* displayed various defects in the first two whorls of flowers, such as extra and fused sepals, as well as loss of or aberrant petals (Krizek et al., 2006; Takeda et al., 2004) (Tables 1, 2; Fig. 4B,C; supplementary material Fig. S4). These phenotypes indicate that RBE controls multiple biological processes during sepal and petal development. To evaluate the role of *MIR164c* in RBE-dependent developmental processes, we examined the genetic interactions of *RBE* with *MIR164c* through double-mutant analyses. The most striking floral phenotype of the *mir164c-1* (*eep1*) mutant was the presence of extra petals in early-arising flowers (Baker et al., 2005) (Fig. 4D,E). In addition, we also observed morphological abnormalities in the second whorl of *eep1* flowers, including aberrantly formed petals and petal filaments (Fig. 4F,G). Plants mutant for *eep1* also occasionally produced extra sepals (supplementary material Fig. S5; Table 2). In the *eep1 rbe-3* double mutant, flowers exhibited complex phenotypes, mainly in the first and second whorls. In the first whorl, the extra sepal phenotype that occurs at a low frequency in both *eep1* and *rbe-3* flowers was enhanced in the double mutant. The *eep1 rbe-3* flowers had significantly more sepals than either single mutant (supplementary material Fig. S5) with extra sepals observed in 31% of the flowers, whereas *eep1* and *rbe-3* have only 5% and 8% flowers with extra sepals, respectively (Table 2; $P<0.005$ for both,

Table 1. Extent of sepal fusion in flowers

	Fraction of sepal length exhibiting fusion*					
Genotype	0	0-1/4	1/4-1/2	1/2-3/4	3/4-1	*n*‡
Wild type	100	0	0	0	0	50
rbe-2	93.84	5.69	0.47	0	0	53
rbe-3	89.54	7.84	2.61	0	0	38
mir164a rbe-2	94.31	5.21	0.47	0	0	53
mir164a rbe-3	90.99	7.11	1.90	0	0	53
eep1 rbe-3	100	0	0	0	0	51
cuc1-1	63.24	20.59	13.24	2.94	0	34
cuc2-1	61.19	16.42	16.43	5.97	0	34
cuc1-1 rbe-3	59.35	22.76	11.38	5.69	0.81	31
cuc2-1 rbe-3	40.54	14.19	23.65	8.11	13.51	37
35S:MIR164b	0	1.96	15.69	43.79	38.56	41
pCUC1:CUC1 rbe-3	90.15	6.90	2.96	0	0	51
pCUC2:CUC2 rbe-3	89.16	8.37	2.46	0	0	51
pCUC1:CUC1m rbe-3	100	0	0	0	0	61
pCUC2:CUC2m rbe-3	98.02	1.49	0.49	0	0	51

*Numbers represent the percentage of sepals exhibiting a given sepal fusion extent.
‡*n*=number of flowers scored.

Fisher's Exact Test). We also observed a novel phenotype, pale green to white sepals with a partial homeotic transformation to second whorl identity, in the first whorl of *eep1 rbe-3* flowers, which was not found in either single mutant (Fig. 4H; Table 2; supplementary material Fig. S6).

The sepal fusion phenotype of *rbe-3* was largely rescued by *eep1* (Table 1), which is consistent with the observation that RBE represses *MIR164c* expression in sepal primordia (Fig. 2). A similar rescue of the *rbe-3* phenotype was also observed in the second whorl of *eep1 rbe-3*. The total second whorl organ number of *eep1 rbe-3* was nearly the same as that of *eep1*, although normal petal number in *eep1 rbe-3* was intermediate to that of the single mutants (supplementary material Fig. S5). In addition, the petal abnormalities present in *rbe-3* flowers were still found in *eep1 rbe-3* (Fig. 4H,I). Together, these results indicate that upregulation of *MIR164c* can account for the absence of petals and sepal fusion defects in *rbe-3*, but might not be the cause of other morphological abnormalities in *rbe-3* mutants.

RBE also regulates *MIR164a* and *MIR164b* expression

Mature miR164 is transcribed from three different loci: *MIR164a*, *b* and *c* (Baker et al., 2005; Sieber et al., 2007). However, *MIR164a* and *MIR164b* expression levels were not significantly affected in DEX-treated *35S:GR-RBE* flowers as shown by both RNA-seq and qPCR (Fig. 1; supplementary material Table S1). Furthermore, we did not observe any enrichment for *MIR164a* or *MIR164b* promoter fragments in *35S:GR-RBE* ChIP analyses (supplementary material Fig. S7), indicating that it is unlikely that RBE regulates *MIR164a* or *MIR164b* expression directly. However, given that the three miR164 genes exhibit redundant functions in flower development (Sieber et al., 2007), it remains to be seen whether RBE also regulates *MIR164a* and *MIR164b* expression indirectly. To test this hypothesis, we examined the expression of promoter-GUS reporters for these two genes (*pMIR164a:GUS* and *pMIR164b:GUS*) in *rbe-3* and wild-type backgrounds. Consistent with previous studies (Sieber et al., 2007), we observed that *MIR164a* and *MIR164b* have distinct expression patterns in wild-type flowers. Specifically, *MIR164a* was expressed in the boundaries between the inflorescence meristem and floral buds, and in stage 2-3 flowers (Fig. 2A,G). Its expression then became largely restricted to the stamens and carpels in later stages (Fig. 2A; supplementary material Fig. S2). At stage 12, *pMIR164a:GUS* expression was observed in the style, the septum and in some cells adjacent to the septum (supplementary material Fig. S2). By contrast, *pMIR164b:GUS* expression was not apparent until stage 6 and was detected predominantly in the sepals and carpels in later flowers (Fig. 2B,H,I; supplementary material Fig. S2). In stage 12 flowers, *MIR164b* displayed a distinct expression pattern in the carpel, with no expression in the septum (supplementary material Fig. S2).

In *rbe-3* flowers, both GUS reporter lines displayed stage-specific changes in their expression patterns. For *pMIR164a:GUS*, we detected reduced GUS expression in stage 2-3 *rbe-3* flowers (Fig. 2D,J), but not in older flowers (supplementary material Fig. S2). This reduction of expression is consistent with qPCR assays (Fig. 3) and suggests that RBE positively regulates *MIR164a* in young floral buds. Positive regulation of *MIR164a* by RBE is also consistent with the *mir164a rbe-2* and *mir164a rbe-3* double-mutant phenotypes. The *rbe-2* allele is a strong loss-of-function mutation in the Col-0 background, resulting from a T-DNA insertion within the coding region (Takeda et al., 2004). Plants that were mutant for *rbe-2* displayed a severe phenotype, with frequent

Table 2. Aberrant sepals in flowers

Genotype	Pale green sepal*	Extra sepal‡	*n*
Wild type	0	0	50
mir164a	0	0	50
eep1	0	5	43
rbe-3	0	7.5	80
mir164ac	20	24	50
mir164a rbe-3	0	6	50
eep1 rbe-3	7.14	30.95	42
pCUC1:CUC1	0	0	51
pCUC2:CUC2	0	0	51
pCUC1:CUC1m	11.76	19.61	51
pCUC2:CUC2m	0	0	51
pCUC1:CUC1 rbe-3	0	11.76	51
pCUC2:CUC2 rbe-3	0	9.80	51
pCUC1:CUC1m rbe-3	11.48	29.51	51
pCUC2:CUC2m rbe-3	0	19.61	51

*Numbers represent the percentage of flowers with pale green sepals.
‡Numbers represent the percentage of flowers with extra sepals.

Fig. 4. Genetic interactions of *RBE* and miR164 genes. (**A-C**) Wild-type (A) and *rbe-3* (B,C) flowers. Arrow in C indicates sepal fusion. (**D-G**) *mir164c* (*eep1*) flowers. In F, one sepal was removed to show aberrant petals (arrows). In G, all four sepals were removed to show filamentous petals (arrow). (**H**,**I**) *eep1 rbe-3* flowers. Arrows in H indicate petal filament and stamenoid petal (from left to right). Arrowhead in H indicates a pale green sepal. Arrows in I indicate aberrant petals (two sepals removed). (**J-Q**) Flowers of *mir164a* (J,K), *mir164a rbe-3* (L), *rbe-2* (M), *mir164a rbe-2* (N), *mir164b* (O), *mir164ab* (P) and *mir164bc* (Q). One sepal was removed in M and N to show filamentous petals (arrow). (**R**,**S**) *mir164ac* flowers. Arrow in R indicates pale green sepals. Arrow in S indicated deformed sepals. (**T**) *35S:MIR164b* flower. Arrows indicate sepal fusions.

conversion of petals into filaments, or exhibiting a lack of petals altogether (Fig. 4M). Plants mutant for *rbe-2* also had sepal fusion defects (Table 1). Double *mir164a-4 rbe-2* or *mir164a-4 rbe-3* mutant flowers largely resembled those of *rbe-2* or *rbe-3*, which is consistent with the hypothesis that RBE acts upstream of and promotes the expression of *MIR164a* (Fig. 4L,N; Table 1). By contrast, the levels of *MIR164b* were found to be slightly increased in *rbe-3* by qPCR (Fig. 3). The patterns of *pMIR164b:GUS* expression indicate that this increase was likely to be due to the precocious or increased expression of *MIR164b* in stage 4-6 flowers of *rbe-3*, compared with that in L *er* at comparable stages (Fig. 2E,K,L). We did not observe any obvious difference in *pMR164b:GUS* expression between *rbe-3* and L *er* in older flowers (supplementary material Fig. S2). These results indicate that RBE also negatively regulates *MIR164b* at specific stages of flower development.

Because the partially redundant functions of miR164 genes are likely to be due to their overlapping patterns of expression in the flower (Sieber et al., 2007), we tested the extent to which the combined activities of the miR164 genes were responsible for different aspects of floral patterning. The *mir164a-4* single mutant had serrated leaves, but showed no obvious floral defects (Nikovics et al., 2006; Sieber et al., 2007) (Fig. 4J,K). The *mir164b-1* mutant displayed a wild-type phenotype in both leaves and flowers (Baker et al., 2005; Sieber et al., 2007) (Fig. 4O). The double *mir164ab* mutants formed normal floral organs as expected (Fig. 4P) because the *MIR164a* and *MIR164b* expression domains are largely exclusive of each other. The double *mir164bc* mutant resembled *eep1* in that these flowers produced extra petals, but otherwise were similar to wild type (Baker et al., 2005) (Fig. 4Q), suggesting that these genes have discrete functions that are probably related to the considerable differences in their expression patterns.

By contrast, the spatial and temporal expression of *MIR164a* and *MIR164c* overlapped with each other in flowers (Fig. 2; supplementary material Fig. S2). Consistent with this overlap, we observed novel floral phenotypes in *mir164ac* double mutants. The *mir164ac* plants showed an enhanced extra sepal phenotype compared with *eep1*; 24% of *mir164ac* flowers had extra sepals (P=0.008) and 20% possessed pale green sepals reminiscent of the petal-like sepals observed in *eep1 rbe-3* (Fig. 4R; supplementary material Fig. S5; Table 2; P<0.005). The similarity between the *mir164ac* double mutant and the *eep1 rbe-3* double mutant further supports the conclusion that *MIR164a* is downregulated in *rbe-3* mutants. Some of the *mir164ac* sepals also exhibited abnormal shapes (Fig. 4S). In the fourth whorl, *mir164ac* double mutants had unfused carpels (Fig. 4R,S). In the second and third whorls, the *mir164ac* double and *eep1* single mutant flowers displayed similar phenotypes (Fig. 4; data not shown). In addition to these double mutants, we also analyzed the phenotypes of *35S:MIR164b* overexpression lines (Baker et al., 2005). Ubiquitous expression of *MIR164b* resulted in fused sepals, and lack of or abnormal petals in the transgenic flowers (Fig. 4T; supplementary material Fig. S5; Table 1). These phenotypic defects emphasize the importance of maintaining specific expression patterns of each of the miR164 genes for normal floral development. As such, the action of RBE in differentially regulating the expression of all three miR164 genes is likely to be important in controlling the levels and distribution of mature miR164 to ensure normal floral organogenesis.

RBE modulates *CUC1* and *CUC2* functions in flower development

CUC1 and *CUC2* genes are targets of miR164 and expression of miR164 cleavage-resistant *CUC1* or *CUC2* genes have demonstrated that miR164 function is largely mediated through *CUC1* and *CUC2* (Baker et al., 2005; Larue et al., 2009; Laufs et al., 2004; Mallory et al., 2004; Nikovics et al., 2006; Peaucelle et al., 2007; Sieber et al., 2007). As *CUC1* and *CUC2* function serves as a read-out for the combined activities of the miR164 genes, we examined the extent to which RBE functions were dependent on CUC activity. Although RBE has opposite effects on *MIR164a* and *MIR164b* expression (Fig. 3), RBE appears to affect *MIR164b* more profoundly than it affects *MIR164a*, because we found that the mature *miRNA164 a/b* level was upregulated in *rbe-3* mutant flowers (Fig. 3). Thus, an increased level of *miR164a/b* and

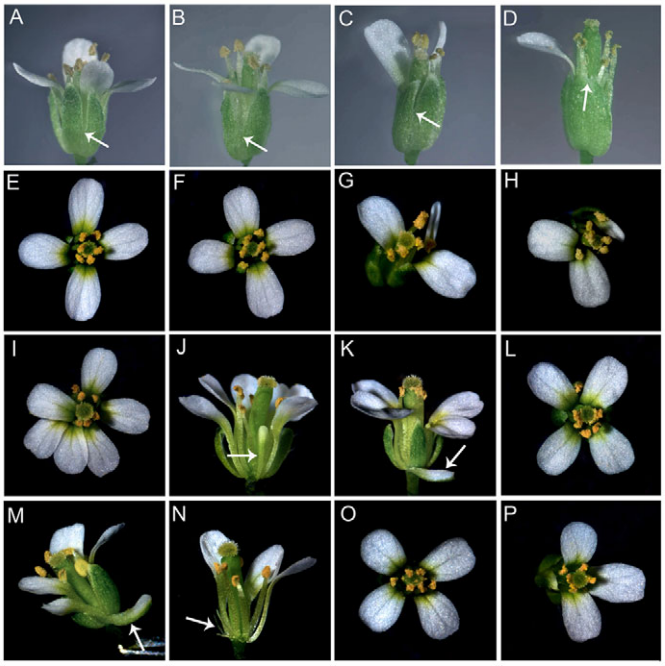

Fig. 5. Genetic interactions of *RBE* with loss-of-function and gain-of-function lines of *CUC1* and *CUC2*. (**A-D**) Flowers of *cuc1-1* (A), *cuc2-1* (B), *cuc1-1 rbe-3* (C) and *cuc2-1 rbe-3* (D). Arrows show the sepal fusion in each flower. Note that sepal fusion is enhanced in *cuc1-1 rbe-3* and *cuc2-1 rbe-3* compared with single mutants. (**E-H**) Flowers of *pCUC1:CUC1* (E), *pCUC2:CUC2* (F), *rbe-3 pCUC1:CUC1* (G) and *rbe-3 pCUC2:CUC2* (H). (**I-K**) *pCUC1:CUC1^m* flowers. Sepals were removed to show the aberrant petal (arrow) in J. The arrow in K indicates the pale green sepal. (**L**) *pCUC2:CUC2^m* flower. (**M**,**N**) *rbe-3 pCUC1:CUC1^m* flowers. The arrow in M indicates the pale green sepal. The sepals were removed in N to show filamentous petals (arrow). (**O**,**P**) Complete (O) and partial (P) rescue of *rbe-3* defects in *rbe-3 pCUC2:CUC2^m* flowers.

MIR164c leads to an overall upregulation of miRNA164 expression in the *rbe-3* mutant. Consistent with this upregulation, we observed a decrease in mRNA abundance of *CUC1* and *CUC2* in *rbe-3* relative to wild type (Fig. 3). Furthermore, in four-hour DEX-induced *35S:GR-RBE* floral tissues, we detected a mild upregulation of *CUC1* and *CUC2* expression compared with mock-treated controls (Fig. 1E).

To determine the extent to which regulation of *CUC1* and *CUC2* activity reflected the biological role of *RBE*, we introduced *rbe-3* into the *cuc1-1* and *cuc2-1* mutant backgrounds. Although with our sample sizes it was not yet statistically significant (P>0.05), both *cuc1-1 rbe-3* and *cuc2-1 rbe-3* exhibited enhanced sepal fusion and more extensive petal defects than in each of the single mutants (Fig. 5A-D; supplementary material Fig. S8; Table 1). Our observation of enhanced sepal fusion in the *cuc2-1 rbe-3* double mutant is also consistent with previous reports (Krizek et al., 2006). The number of mis-shapen petals and the extent of sepal fusion were comparable to the phenotypes seen in *35S:MIR164b* plants, in which *CUC1* and *CUC2* expression levels are simultaneously reduced (supplementary material Figs S5, S8; Table 1). These observations support our expression data that *CUC1* and *CUC2* levels are both reduced in *rbe-3* (Fig. 2).

We also tested the effect of overexpressing *CUC1* or *CUC2* in *rbe-3* by introducing miR164-resistant versions of *CUC1* or *CUC2* (*CUC1^m* or *CUC2^m*) driven by their native promoters into the *rbe-3* mutant. We utilized miR164-sensitive *pCUC1:CUC1* and *pCUC2:CUC2* lines as controls. *pCUC:CUC1* and *pCUC2:CUC2* both displayed wild-type floral organs owing to post-transcriptional regulation by endogenous miR164 (Baker et al., 2005), whereas *rbe-3 pCUC1:CUC1* and *rbe-3 pCUC2:CUC2* flowers resembled those of *rbe-3* in organ number and morphology (Fig. 5E-H; supplementary material Fig. S8; Tables 1, 2). Similar to what has been previously reported (Baker et al., 2005), we observed phenotypes in *pCUC1:CUC1^m* plants that mimic those of the *eep1* mutant. These phenotypes included extra petals in the second whorl, as well as extra sepals in the first whorl (Fig. 5I-K; supplementary material Fig. S8; Table 2). However, we also observed that the extra sepal phenotype appeared to be more pronounced in *pCUC1:CUC1^m* flowers compared with *eep1* (20% in *pCUC1:CUC1^m* compared with 5% in *eep1*; Table 2; P=0.03). Furthermore, we also found that the *pCUC1:CUC1^m* flowers frequently displayed pale green to white sepals that were reminiscent of those seen in *mir164ac* and *eep1 rbe-3* flowers (Fig. 5K; Table 2; P=0.02). These observations suggest that the subtle differences between the *pCUC1:CUC1^m* and *eep1* flowers are due to an excess accumulation of *CUC1* gene product in the *pCUC1:CUC1^m* plants that occurs because of the lack of *miR164a*- and *miR164b*-mediated degradation. Furthermore, many of the *rbe* phenotypes were rescued in the *pCUC1:CUC1^m* background. These included first whorl sepal fusion that is seen in *rbe-3* mutants but is completely ameliorated in *rbe-3 pCUC1:CUC1^m* plants (Table 1). In the second whorl, the total organ number in *rbe-3 pCUC1:CUC1^m* was equivalent to that seen in *pCUC1:CUC1^m* plants, whereas the petal morphology defects in *rbe-3* were partially rescued in *rbe-3 pCUC1:CUC1^m* plants (Fig. 5M,N; supplementary material Fig. S8). The only synergistic interaction found in *rbe-3 pCUC1:CUC1^m* plants was the increased sepal number compared with the parental *pCUC1:CUC1^m* and *rbe-3* single mutants (supplementary material Fig. S8; Table 2; P=0.09 and P=0.009, respectively), which suggests that the extra sepal phenotype in *rbe-3* is at least partly due to processes independent of the miR164-CUC pathway. This idea is also supported by the observation that *rbe-3 pCUC2:CUC2^m* also displayed an enhanced extra sepal phenotype compared with the parental *rbe-3* and *pCUC2:CUC2^m* single mutants (Table 2; P=0.04 and P<0.005, respectively).

Although not showing strong floral phenotypes on its own, the *pCUC2:CUC2^m* construct could partially compensate for the floral defects of *rbe-3* in the *rbe-3 pCUC2:CUC2^m* combination. In the first whorl, the sepal fusion defect of *rbe-3* appeared to be ameliorated in the *rbe-3 pCUC2:CUC2^m* plants, indicating a partial rescue of the *rbe* mutant phenotype (Table 1; P=0.09). In the second whorl, *rbe-3 pCUC2:CUC2^m* plants displayed considerably more normal petals than seen in *rbe-3* flowers (Fig. 5O,P; supplementary material Fig. S8). Together, our results demonstrate that *RBE* activates *CUC1* and *CUC2* at least in part by modulating the expression of multiple miR164 genes.

DISCUSSION

In this study, we demonstrated that RBE can bind to the promoter of, and regulate the expression of, *MIR164c*. RBE also regulates the expression of *MIR164a* and *MIR164b*, although this appears to be indirect. The transcriptional regulation of the miR164 genes by RBE appears to be important in defining both the localization and timing of mature miR164 accumulation that, in turn, impacts CUC-dependent boundary specification and concomitant organogenesis.

RBE represents a novel control point in the regulation of miR164-mediated developmental processes

The *CUC1* and *CUC2* genes are redundantly required for the formation of tissue boundaries as well as for the repression of growth in a variety of tissues. These instances of boundary formation and repression of growth include cotyledon separation during embryogenesis, lateral organ initiation on the flanks of the shoot apical meristem, and leaf margin serration, indicating that a similar mechanism operates to establish boundaries in these different contexts (Aida et al., 1997; Aida et al., 1999; Heisler et al., 2005; Hibara et al., 2006; Laufs et al., 2004; Nikovics et al., 2006; Raman et al., 2008; Takada et al., 2001; Vroemen et al., 2003). In all of these tissues, post-transcriptional regulation of the *CUC1* and *CUC2* genes by miR164 is a key regulatory mechanism controlling CUC gene expression levels and consequent regulation of growth (Baker et al., 2005; Larue et al., 2009; Laufs et al., 2004; Mallory et al., 2004; Nikovics et al., 2006; Peaucelle et al., 2007; Sieber et al., 2007). However, to date, relatively little is known about how miRNA genes themselves are regulated to effect particular developmental outcomes through the production of a single mature miRNA species. For instance, in *Arabidopsis*, miR172 is encoded by five genes, and transcription factors binding to promoter regions of individual miR172 genes have been identified (Grigorova et al., 2011; Wu et al., 2009; Yant et al., 2010). However, the mechanisms for coordinately regulating the family of miR172 genes are not yet clear. *GIGANTEA* (*GI*) has been shown to regulate overall miR172 abundance, but this regulation appears to occur via GI-mediated processing of miR172, rather than through transcriptional control, and might not be specific to miR172 (Jung et al., 2007).

Direct promotion of the expression of *MIR164a* by the TCP3 transcription factor has been shown to lead to downregulation of the *CUC1* and *CUC2* genes during leaf differentiation (Koyama et al., 2007; Koyama et al., 2010). TCP3 also regulates a suite of genes involved in auxin signaling, which in turn provides a mechanism for feedback control on the expression of the CUC genes (Koyama et al., 2010). RBE, by contrast, appears to act in a distinct manner, via the transcriptional control of all three miR164 genes, with *MIR164c* being directly repressed by RBE during sepal and petal development.

MIR164a and *MIR164c* have partially redundant functions in that the double *mir164ac* mutant displays extra sepals, mis-shapen sepals, and chimeric sepal-petal organs not seen in either single mutant (Fig. 4; supplementary material Fig. S5). These phenotypes were also seen in double mutant combinations of *mir164c* with *rbe-3*, supporting the idea that RBE positively regulates *MIR164a*. Furthermore, this result suggests that RBE might have a non-autonomous function in regulating sepal primordium initiation. Our results indicate that *MIR164c* is directly repressed by RBE in stages 3-5 flowers. Consistent with this result, we observed various petal defects in *rbe-3* that can be partially or completely rescued by the loss of *MIR164c* (Fig. 4). *MIR164b* transcription is also repressed by RBE during this period, and its premature expression in the *rbe* mutant probably also contributes to the petal defects we observe. However, it is also clear that RBE acts to regulate many other genes that are likely to impact the development of sepal and petal primordia (supplementary material Table S1). RBE has been reported to negatively regulate the expression of the *AGAMOUS* (*AG*) floral homeotic gene and restrict its expression from the second whorl (Krizek et al., 2006). Although we did not identify *AG* as a significantly downregulated gene in DEX-induced *35S:GR-RBE* plants (supplementary material Table S1), potentially the ectopic expression of *AG* in the second whorl of *rbe* mutant plants could be a contributing factor to the observed defects in petal primordium initiation and growth.

Our genetic analyses indicate that CUC1 and CUC2 are major effectors of RBE activity, as *pCUC1:CUC1*^{m}, and to a lesser extent, *pCUC2:CUC2*^{m}, can suppress many aspects of the *rbe* mutant phenotype. Through regulating the expression of the miR164 genes, RBE can fine-tune the expression of the CUC genes to precisely define the proliferative capabilities of different domains of cells. Alterations in RBE and/or miR164 function through single and double mutant combinations indicate that one consequence of disrupting normal levels of CUC activity is the formation of ectopic boundaries, mis-specified boundaries, and lack of normal boundary formation. As RBE acts independently of organ identity specification (Takeda et al., 2004), these mutant effects on boundary formation can lead to the formation of primordia that incorporate cells from normally distinct whorls, resulting in chimeric organs. Also, it is clear that miR164 gene activity also is required for CUC-independent organ formation (Baker et al., 2005), suggesting that RBE probably controls other aspects of organ formation, at least in part, through regulating miR164 spatial and temporal expression patterns that regulate CUC-independent processes.

Coordinate control of multiple miRNAs

In contrast to most animal miRNAs, plant miRNAs are usually transcribed from large gene families consisting of multiple miRNA precursors (Li and Mao, 2007). Similar to protein-coding gene families, miRNA gene families, including the miR164 genes, probably originated from gene or genome duplications, and subsequently underwent functional diversification to acquire specific biological functions (Maher et al., 2006). Because miRNA gene families usually produce similar or identical mature miRNAs, the functional specificity of each miRNA gene largely results from its distinct spatial and temporal expression pattern. For instance, the maize miR166 gene family includes nine members that are localized in distinct patterns in the shoot apex, with only some of these genes contributing to the function of miR166 in the specification of the abaxial side of leaves (Nogueira et al., 2009).

Jasinski et al. (Jasinski et al., 2010) have shown that the miR164 genes appear to have evolved in a stepwise manner, with the *MIR164b* lineage probably pre-dating the radiation of the angiosperms, and a more recent duplication giving rise to the *MIR164a* and *MIR164c* gene lineages present in *Arabidopsis*. Consistent with these evolutionary relationships, *MIR164a* and *MIR164c* display partially overlapping expression patterns, whereas *MIR164b* exhibits a distinct pattern in both early and late stage flowers (Fig. 2; supplementary material Fig. S2). These separate derivations imply that the regulatory control of each miR164 gene also evolved independently. Our observations that RBE regulates the two most closely related *Arabidopsis* miR164 genes differently supports this idea and implies that these RBE-dependent pathways were either independently recruited to this regulatory role or that the regulation of each gene diversified while maintaining an overall RBE-dependent regulatory logic.

Although RBE appears to directly and negatively regulate *MIR164c* expression in sepal and petal primordia during early stages of floral development, it is still unclear how miR164 gene expression is modulated in other tissues and at other times. Like *RBE*, *SUPERMAN* (*SUP*) encodes a putative EPF-type zinc finger transcriptional repressor and has been postulated to regulate the

formation of the boundary between stamen and carpel whorls in the flower (Sakai et al., 1995). One tantalizing possibility is that SUP, and potentially other related EPF-type zinc finger proteins, act similarly to RBE to regulate miR164 gene expression in order to control CUC activity at other boundary domains.

Acknowledgements
We thank Drs Elliot Meyerowitz and Patrick Laufs for gifts of seed stocks, and Dr Kathy Barton for a gift of the *pJAN33* plasmid.

Funding
T.H. was supported in part through a Yale University Brown Fellowship. This project was supported by a National Science Foundation grant [IOS-0817744 to V.F.I.].

Competing interests statement
The authors declare no competing financial interests.

Supplementary material
Supplementary material available online at
http://dev.biologists.org/lookup/suppl/doi:10.1242/dev.075069/-/DC1

References

Aida, M. and Tasaka, M. (2006). Genetic control of shoot organ boundaries. *Curr. Opin. Plant Biol.* **9**, 72-77.
Aida, M., Ishida, T., Fukaki, H., Fujisawa, H. and Tasaka, M. (1997). Genes involved in organ separation in Arabidopsis: an analysis of the cup-shaped cotyledon mutant. *Plant Cell* **9**, 841-857.
Aida, M., Ishida, T. and Tasaka, M. (1999). Shoot apical meristem and cotyledon formation during Arabidopsis embryogenesis: interaction among the CUP-SHAPED COTYLEDON and SHOOT MERISTEMLESS genes. *Development* **126**, 1563-1570.
Baker, C. C., Sieber, P., Wellmer, F. and Meyerowitz, E. M. (2005). The early extra petals1 mutant uncovers a role for microRNA miR164c in regulating petal number in Arabidopsis. *Curr. Biol.* **15**, 303-315.
Bonnet, E., Wuyts, J., Rouze, P. and Van de Peer, Y. (2004). Detection of 91 potential conserved plant microRNAs in Arabidopsis thaliana and Oryza sativa identifies important target genes. *Proc. Natl. Acad. Sci. USA* **101**, 11511-11516.
Chen, C., Ridzon, D. A., Broomer, A. J., Zhou, Z., Lee, D. H., Nguyen, J. T., Barbisin, M., Xu, N. L., Mahuvakar, V. R., Andersen, M. R. et al. (2005). Real-time quantification of microRNAs by stem-loop RT-PCR. *Nucleic Acids Res.* **33**, e179.
Clough, S. J. and Bent, A. F. (1998). Floral dip: A simplified method for Agrobacterium-mediated transformation of Arabidopsis thaliana. *Plant J.* **16**, 735-743.
Dahmann, C., Oates, A. C. and Brand, M. (2011). Boundary formation and maintenance in tissue development. *Nat. Rev. Genet.* **12**, 43-55.
Gendrel, A. V., Lippman, Z., Yordan, C., Colot, V. and Martienssen, R. A. (2002). Dependence of heterochromatic histone H3 methylation patterns on the Arabidopsis gene DDM1. *Science* **297**, 1871-1873.
Grigorova, B., Mara, C., Hollender, C., Sijacic, P., Chen, X. and Liu, Z. (2011). LEUNIG and SEUSS co-repressors regulate miR172 expression in Arabidopsis flowers. *Development* **138**, 2451-2456.
Heisler, M. G., Ohno, C., Das, P., Sieber, P., Reddy, G. V., Long, J. A. and Meyerowitz, E. M. (2005). Patterns of auxin transport and gene expression during primordium development revealed by live imaging of the Arabidopsis inflorescence meristem. *Curr. Biol.* **15**, 1899-1911.
Hibara, K., Karim, M. R., Takada, S., Taoka, K., Furutani, M., Aida, M. and Tasaka, M. (2006). Arabidopsis CUP-SHAPED COTYLEDON3 regulates postembryonic shoot meristem and organ boundary formation. *Plant Cell* **18**, 2946-2957.
Irish, V. F. (2008). The Arabidopsis petal: a model for plant organogenesis. *Trends Plant Sci.* **13**, 430-436.
Jasinski, S., Vialette-Guiraud, A. C. and Scutt, C. P. (2010). The evolutionary-developmental analysis of plant microRNAs. *Philos. Trans. R. Soc. Lond. B Biol. Sci.* **365**, 469-476.
Jones-Rhoades, M. W. and Bartel, D. P. (2004). Computational identification of plant microRNAs and their targets, including a stress-induced miRNA. *Mol. Cell* **14**, 787-799.
Jung, J. H., Seo, Y. H., Seo, P. J., Reyes, J. L., Yun, J., Chua, N. H. and Park, C. M. (2007). The GIGANTEA-regulated microRNA172 mediates photoperiodic flowering independent of CONSTANS in Arabidopsis. *Plant Cell* **19**, 2736-2748.
Koyama, T., Furutani, M., Tasaka, M. and Ohme-Takagi, M. (2007). TCP transcription factors control the morphology of shoot lateral organs via negative regulation of the expression of boundary-specific genes in Arabidopsis. *Plant Cell* **19**, 473-484.
Koyama, T., Mitsuda, N., Seki, M., Shinozaki, K. and Ohme-Takagi, M. (2010). TCP transcription factors regulate the activities of ASYMMETRIC LEAVES1 and miR164, as well as the auxin response, during differentiation of leaves in Arabidopsis. *Plant Cell* **22**, 3574-3588.
Krizek, B. A., Lewis, M. W. and Fletcher, J. C. (2006). RABBIT EARS is a second-whorl repressor of AGAMOUS that maintains spatial boundaries in Arabidopsis flowers. *Plant J.* **45**, 369-383.
Larue, C. T., Wen, J. and Walker, J. C. (2009). A microRNA-transcription factor module regulates lateral organ size and patterning in Arabidopsis. *Plant J.* **58**, 450-463.
Laufs, P., Peaucelle, A., Morin, H. and Traas, J. (2004). MicroRNA regulation of the CUC genes is required for boundary size control in Arabidopsis meristems. *Development* **131**, 4311-4322.
Li, A. and Mao, L. (2007). Evolution of plant microRNA gene families. *Cell Res.* **17**, 212-218.
Maher, C., Stein, L. and Ware, D. (2006). Evolution of Arabidopsis microRNA families through duplication events. *Genome Res.* **16**, 510-519.
Mallory, A. C., Dugas, D. V., Bartel, D. P. and Bartel, B. (2004). MicroRNA regulation of NAC-domain targets is required for proper formation and separation of adjacent embryonic, vegetative, and floral organs. *Curr. Biol.* **14**, 1035-1046.
Nakayama, N., Arroyo, J. M., Simorowski, J., May, B., Martienssen, R. and Irish, V. F. (2005). Gene trap lines define domains of gene regulation in Arabidopsis petals and stamens. *Plant Cell* **17**, 2486-2506.
Neff, M. M., Neff, J. D., Chory, J. and Pepper, A. E. (1998). dCAPS, a simple technique for the genetic analysis of single nucleotide polymorphisms: experimental applications in Arabidopsis thaliana genetics. *Plant J.* **14**, 387-392.
Nikovics, K., Blein, T., Peaucelle, A., Ishida, T., Morin, H., Aida, M. and Laufs, P. (2006). The balance between the MIR164A and CUC2 genes controls leaf margin serration in Arabidopsis. *Plant Cell* **18**, 2929-2945.
Nogueira, F. T., Chitwood, D. H., Madi, S., Ohtsu, K., Schnable, P. S., Scanlon, M. J. and Timmermans, M. C. (2009). Regulation of small RNA accumulation in the maize shoot apex. *PLoS Genet.* **5**, e1000320.
Peaucelle, A., Morin, H., Traas, J. and Laufs, P. (2007). Plants expressing a miR164-resistant CUC2 gene reveal the importance of post-meristematic maintenance of phyllotaxy in Arabidopsis. *Development* **134**, 1045-1050.
Raman, S., Greb, T., Peaucelle, A., Blein, T., Laufs, P. and Theres, K. (2008). Interplay of miR164, CUP-SHAPED COTYLEDON genes and LATERAL SUPPRESSOR controls axillary meristem formation in Arabidopsis thaliana. *Plant J.* **55**, 65-76.
Reinhart, B. J., Weinstein, E. G., Rhoades, M. W., Bartel, B. and Bartel, D. P. (2002). MicroRNAs in plants. *Genes Dev.* **16**, 1616-1626.
Rhoades, M. W., Reinhart, B. J., Lim, L. P., Burge, C. B., Bartel, B. and Bartel, D. P. (2002). Prediction of plant microRNA targets. *Cell* **110**, 513-520.
Sakai, H., Medrano, L. J. and Meyerowitz, E. M. (1995). Role of SUPERMAN in maintaining Arabidopsis floral whorl boundaries. *Nature* **378**, 199-201.
Sieber, P., Wellmer, F., Gheyselinck, J., Riechmann, J. L. and Meyerowitz, E. M. (2007). Redundancy and specialization among plant microRNAs: role of the MIR164 family in developmental robustness. *Development* **134**, 1051-1060.
Takada, S., Hibara, K., Ishida, T. and Tasaka, M. (2001). The CUP-SHAPED COTYLEDON1 gene of Arabidopsis regulates shoot apical meristem formation. *Development* **128**, 1127-1135.
Takeda, S., Matsumoto, N. and Okada, K. (2004). RABBIT EARS, encoding a SUPERMAN-like zinc finger protein, regulates petal development in Arabidopsis thaliana. *Development* **131**, 425-434.
Trapnell, C., Pachter, L. and Salzberg, S. L. (2009). TopHat: discovering splice junctions with RNA-Seq. *Bioinformatics* **25**, 1105-1111.
Vroemen, C. W., Mordhorst, A. P., Albrecht, C., Kwaaitaal, M. A. and de Vries, S. C. (2003). The CUP-SHAPED COTYLEDON3 gene is required for boundary and shoot meristem formation in Arabidopsis. *Plant Cell* **15**, 1563-1577.
Wang, X. J., Reyes, J. L., Chua, N. H. and Gaasterland, T. (2004). Prediction and identification of Arabidopsis thaliana microRNAs and their mRNA targets. *Genome Biol.* **5**, R65.
Wu, G., Park, M. Y., Conway, S. R., Wang, J. W., Weigel, D. and Poethig, R. S. (2009). The sequential action of miR156 and miR172 regulates developmental timing in Arabidopsis. *Cell* **138**, 750-759.
Yant, L., Mathieu, J., Dinh, T. T., Ott, F., Lanz, C., Wollmann, H., Chen, X. and Schmid, M. (2010). Orchestration of the floral transition and floral development in Arabidopsis by the bifunctional transcription factor APETALA2. *Plant Cell* **22**, 2156-2170.
Zhang, Z., Lopez-Giraldez, F. and Townsend, J. P. (2010). LOX: inferring Level Of eXpression from diverse methods of census sequencing. *Bioinformatics* **26**, 1918-1919.